

Supporting Information

for

Solid rheological properties of PBT-based vitrimers

L. Farge^{1*}, S.Hoppe², V. Daujat^{1,2}, F. Tournilhac³, S. André¹

1 Université de Lorraine, CNRS, LEMTA, F-54000 Nancy, France

2 Université de Lorraine, CNRS, LRGP, F-54000 Nancy, France

3 Molecular, Macromolecular Chemistry, and Materials, ESPCI Paris, PSL University, CNRS, 10 Rue Vauquelin, F-75005 Paris, France

Content

1. True strains, true stresses and necking.....	2
2. DSC experiments	3
3. TGA experiments.....	3
4. X-ray diffraction experiments.....	4
5. Additional results obtained from monotonic tensile tests	7
6. Creep tests.....	9
7. Continuous Reactive Extrusion.....	10

1. True strains, true stresses and necking

Definition of the true strain (logarithmic strain)

Let l_0 be a very small length element taken along the drawing axis on the undeformed specimen. During the deformation process, the size of this length element varies and its current size is denoted l . When l changes from l to $l + dl$, the corresponding strain increment is $d\varepsilon = \frac{dl}{l}$. The total strain

or true strain is then given by $\varepsilon = \int d\varepsilon = \int_{l_0}^l \frac{dl}{l} = \ln\left(\frac{l}{l_0}\right)$.

Because l_0 is very small, ε is a local quantity that varies along the specimen length. In the specimen central cross-section, ε is denoted ε^M .

In a similar way, the logarithmic transverse strain in the central cross-section is given by:

$$\varepsilon_t^M = \ln\left(\frac{d}{d_0}\right).$$

d_0 and d are the initial and current dimensions of the central square cross-section respectively. The initial and current areas of the central cross-section are denoted $S_0 = d_0^2$ and $S = d^2$.

Expression of the true stress

The true or Cauchy stress is the actual stress to which the material is subjected during the test. It is given by $\sigma = \frac{F}{S}$

The true stress in the central cross-section can be rewritten as follows:

$$\sigma = \frac{F}{S} = \frac{F}{d^2} = \frac{F}{d_0^2} e^{-2\varepsilon_t^M} = \frac{F}{S_0} e^{-2\varepsilon_t^M}.$$

Assuming an isochoric deformation process: $\frac{ld^2}{l_0 d_0^2} = 1 \Rightarrow \varepsilon^M + 2\varepsilon_t^M = 0$

Using this equation to replace $-2\varepsilon_t^M$ by ε^M in $\sigma = \frac{F}{S_0} e^{-2\varepsilon_t^M}$, we obtain $\sigma = \frac{F}{S_0} e^{\varepsilon^M}$.

In our study, this last equation was used to obtain σ in the central cross-section. During a tensile test, F and ε^M are respectively measured by the force sensor and by image correlation (3D DIC).

For the sake of simplicity, we assumed that the materials are transversely isotropic. However, the expression for σ ($\sigma = \frac{F}{S_0} e^{\varepsilon^M}$) is unchanged if we consider that the central cross-section thickness and width variations are not the same during the test.

Link between the strain-hardening coefficient γ and necking

As indicated in the paper, the strain hardening coefficient is given by: $\gamma(\varepsilon_M) = \frac{d \ln(\sigma)}{d \varepsilon_M}$

If $\frac{dF}{d\varepsilon^M} > 0$ throughout the test, no yield point appears on the force curve.

Starting from $F = \sigma S_0 e^{-\varepsilon^M}$, we can check that :

$$\frac{dF}{d\varepsilon^M} > 0 \Leftrightarrow \frac{d\sigma}{d\varepsilon^M} S_0 e^{-\varepsilon^M} - \sigma S_0 e^{-\varepsilon^M} > 0 \Leftrightarrow \frac{d\sigma}{d\varepsilon^M} > \sigma \Leftrightarrow \frac{\frac{d\sigma}{d\varepsilon^M}}{\sigma} > 1 \Leftrightarrow \gamma = \frac{d \ln(\sigma)}{d \varepsilon^M} > 1$$

This proves that necking occurs only if the intrinsic quantity γ becomes smaller than 1.

2. DSC experiments

Thermal characterization was performed for all the polymers by differential scanning calorimetry (DSC) (Mettler Toledo, DSC 1). Both temperature and heat flow were calibrated using indium and tin standards. The weight of all samples employed was in the range of 9-13 mg. In the DSC measurement, polymer sample was heated at 260°C with a rate of 10.0 K/min and then cooled down to 25 °C with a rate of 10.0 K/min. The melting point (T_m) of crystals in the sample was chosen as the temperature at the peak maximum of melting transition measured in the heating run and the heat of fusion (ΔH_m) was additionally estimated. The glass transition temperature (T_g) was chosen as the temperature at the middle point of glass transition obtained in the heating run. The degree of crystallinity, χ_c , was determined by dividing the melting enthalpy (ΔH_m) of the heating by the melting enthalpy (ΔH_{0m}) for 100% crystalline pristine PBT. For ΔH_{0m} , value of 142 J/g was used in this study.ⁱ

Produit	Pristine PBT	V_1	V_2	PV_1	$PV_{1.3}$	$PV_{1.6}$
T_g (glass transition temperature) °C	50.00	51.4	48.3	47.1	46.7	46.5
T_m (Melting temperature) °C	225	222	224	223.5	221.3	219.7
Melting enthalpy (J/g) (Sandrine)	49.38	45.35	43.30	46.04	42.39	41.05
Cristallinity degree (%)	34.8	31.9	30.5	32.4	29.85	28.9

Table S1 Pristine PBT and vitrimer DSC results

3. TGA experiments

Thermogravimetric (TGA) measurements were carried out using a Netzsch Libra TG209 instrument equipped with a type P thermocouple / ceramic sample carrier. Samples of about 6-11 mg weight placed in disposable aluminum crucibles were subjected to a thermal ramp from 25 to 600°C at 10°C/min under a nitrogen atmosphere.

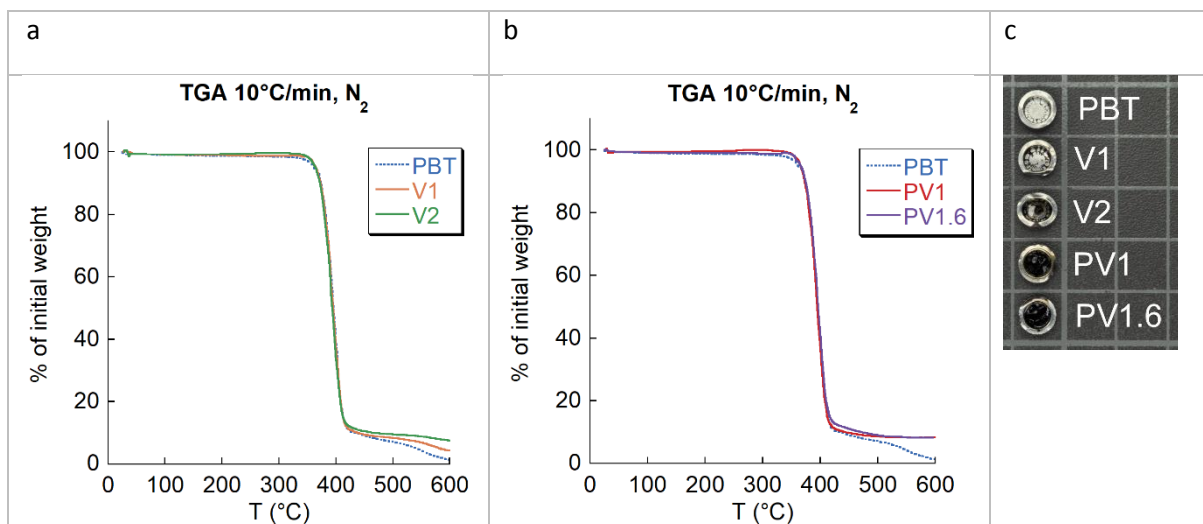


Figure S1 TGA measurements of a) pristine PBT and vitrimers V₁, V₂, b) pristine PBT and previtrimers PV₁ and PV_{1.6}, c) aspect of the char residue after pyrolysis.

4. X-ray diffraction experiments

X-ray diffraction measurements were conducted at DND-CAT beamline (5-ID-D sector) at the advanced Photon Source in Argonne National Laboratory (Argonne, IL, USA).ⁱⁱ Injection molded bars were placed on flat panel sample holders. The X-ray wavelength was 0.729 Å, 2D scattering patterns covering the whole $q = 0.025$ to 4.45 Å^{-1} scattering range were collected using a set of three Rayonix LX170HS CCD area detectors; $I(q)$ plots were then generated by azimuthal averaging of the $q = 0.13$ to 4.45 Å^{-1} range.

For indexing of the Bragg peaks, a sample position correction was applied to take into account the small offset between the center of the specimen and the reference plane. The spectra of pristine PBT and V₂ vitrimer samples are plotted in Fig. S14, together with the expected reflections' positions.

Observed reflexions match the positions calculated using the unit cell dimensions of the α crystalline form of PBTⁱⁱⁱ (Triclinic, $P\bar{1}$ space group, $a = 4.86 \text{ Å}$, $b = 5.96 \text{ Å}$, $c = 11.65 \text{ Å}$, $\alpha = 99.7^\circ$, $\beta = 116.0^\circ$, $\gamma = 110.8^\circ$).

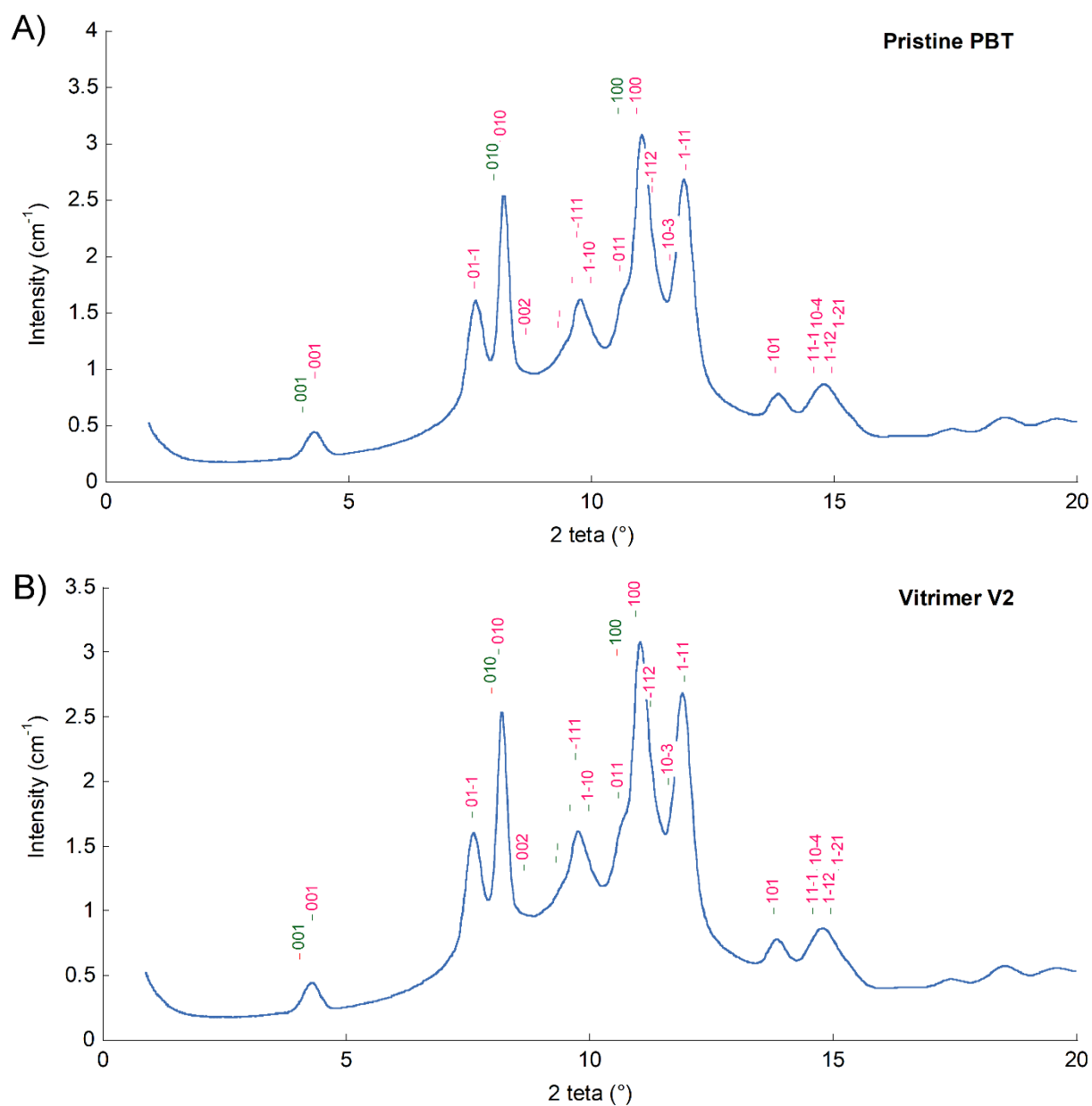
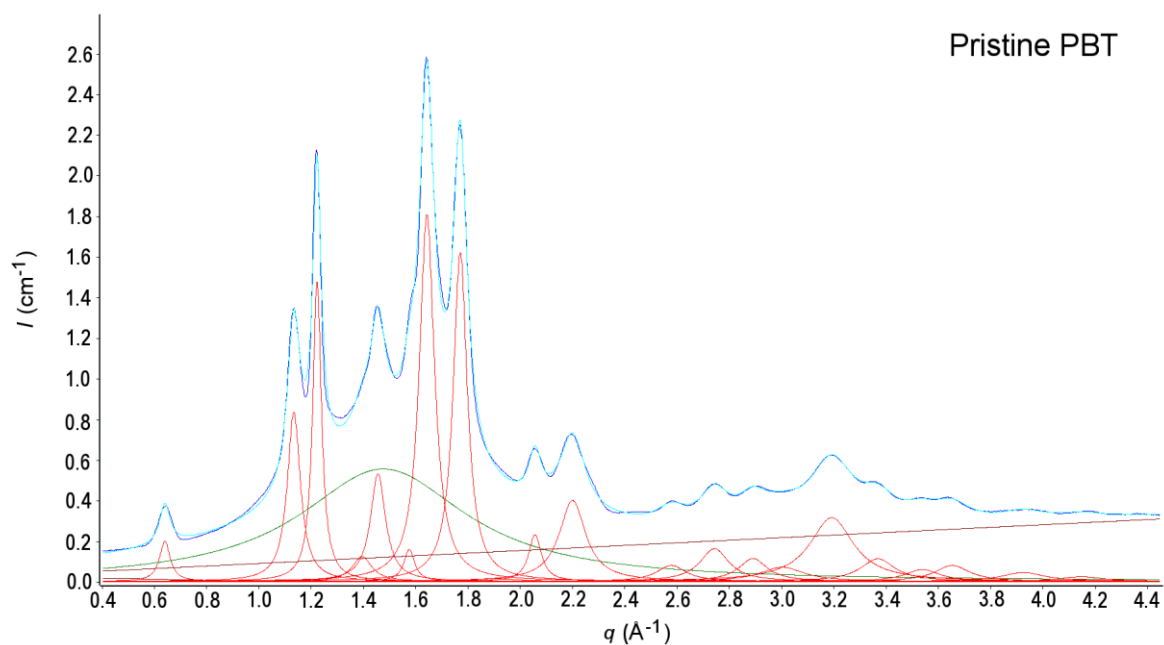


Figure S2 Indexation of A) pristine PBT and B) vitrimer V₂ Debye-Scherrer diagrams. Calculated hkl positions of the triclinic α form are shown in red. Calculated (not observed) positions of the β form are shown in green.

A)



B)

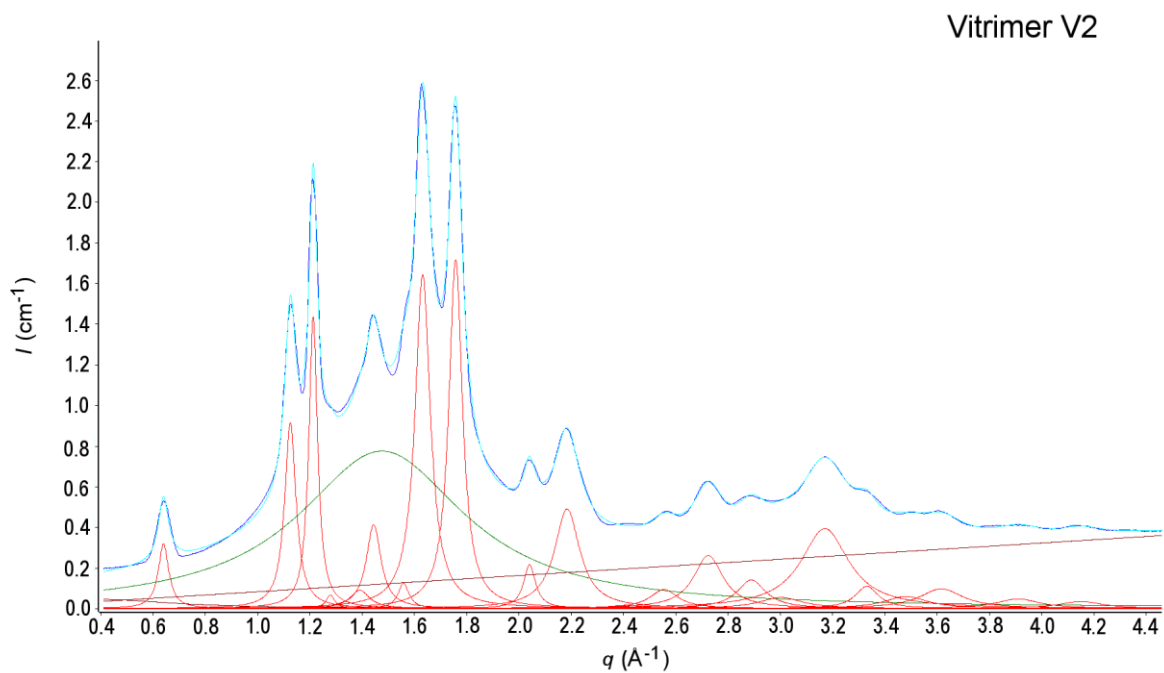


Figure S3 WAXS measurements (in dark blue) of A) pristine PBT and B) vitrimer V2. The decomposition into a sum of Bragg peaks (in red) and a wide diffuse background (in green) is shown. The result of the fit is shown in light blue.

5. Additional results obtained from monotonic tensile tests

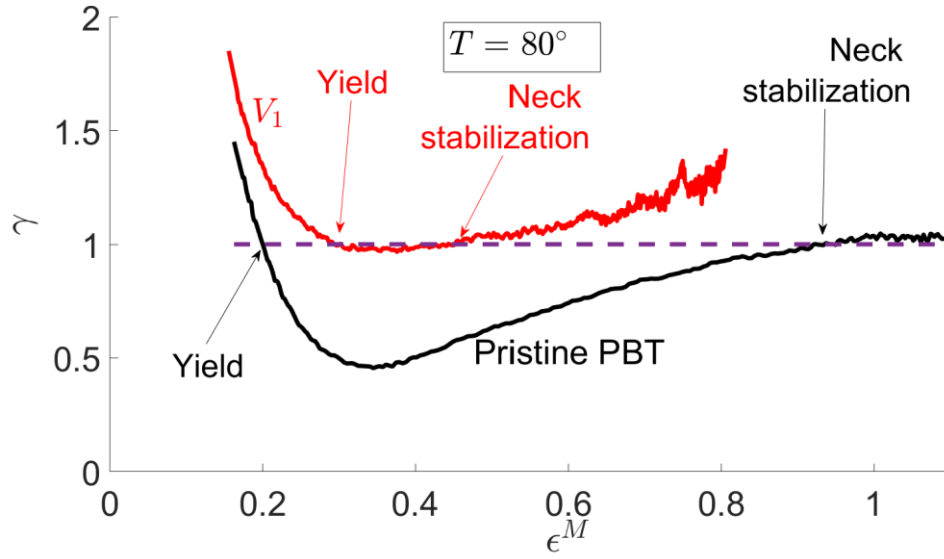


Figure S4 Evolution of the strain-hardening coefficient $\gamma = \frac{d \ln(\sigma)}{d \varepsilon^M}$ at $T = 80^\circ\text{C}$. γ is not represented for V_2 because rupture occurred at $\varepsilon^M \approx 0.15$.

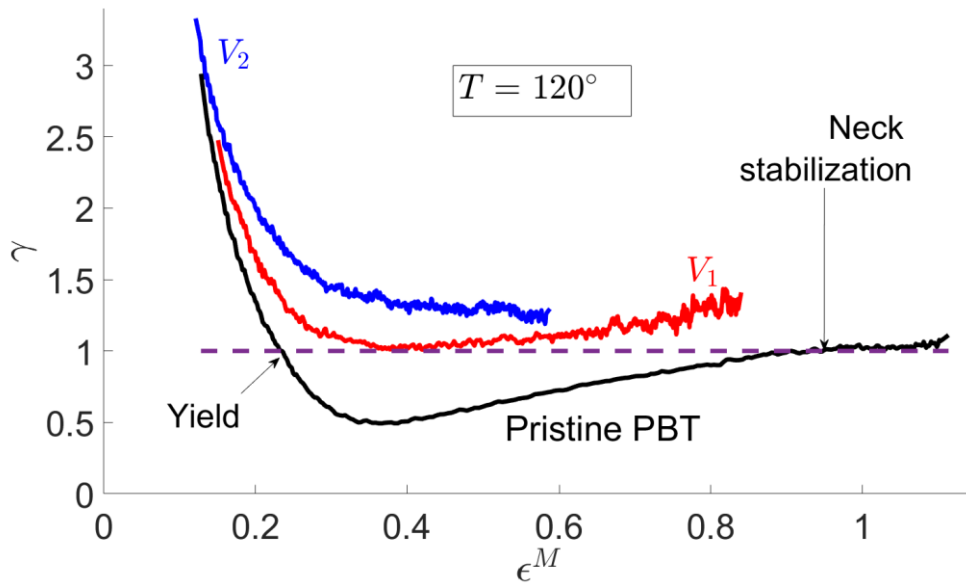


Figure S5 Evolution of the strain-hardening coefficient $\gamma = \frac{d \ln(\sigma)}{d \varepsilon^M}$ at $T = 120^\circ\text{C}$.

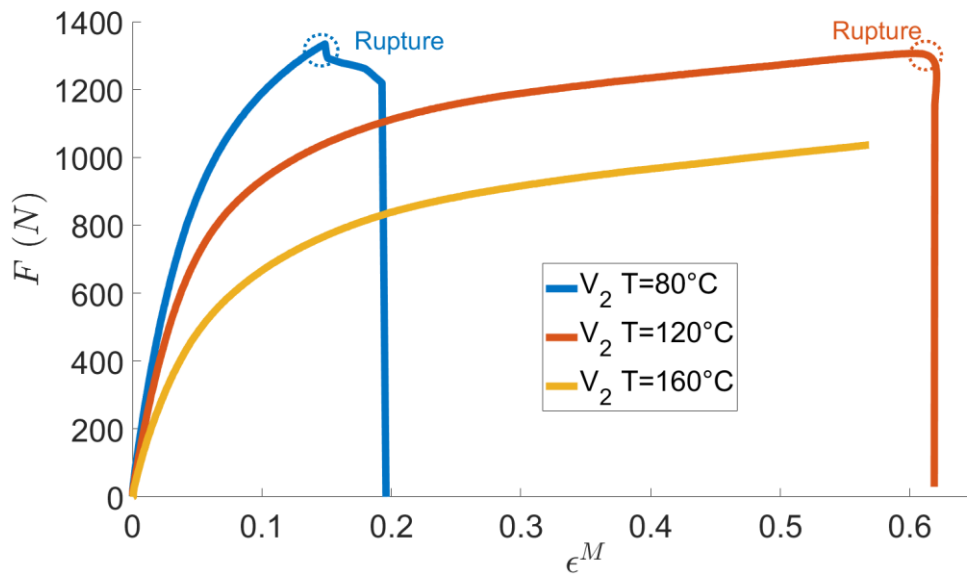


Figure S6 Evolution of the force signals for the V_2 vitrimer at 80°C, 120°C and 160°C .

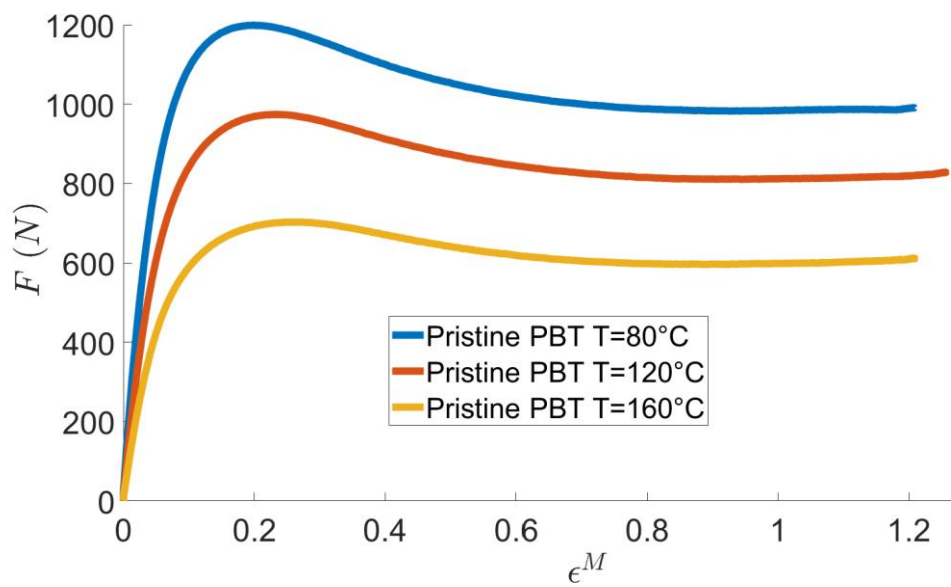


Figure S7 Evolution of the force signals for the pristine PBT at 80°C, 120°C and 160°C .

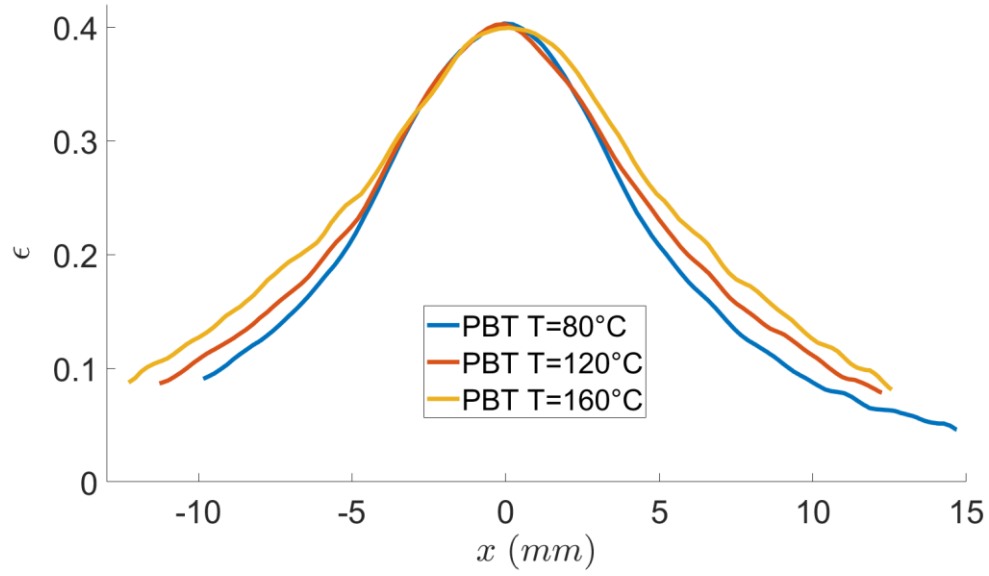


Figure S8 Strain profiles taken at 80°C, 120°C and 160°C along the specimen central axis for the pristine PBT. The measurements were made when the strain in the specimen center was $\varepsilon^M = 0.4$.

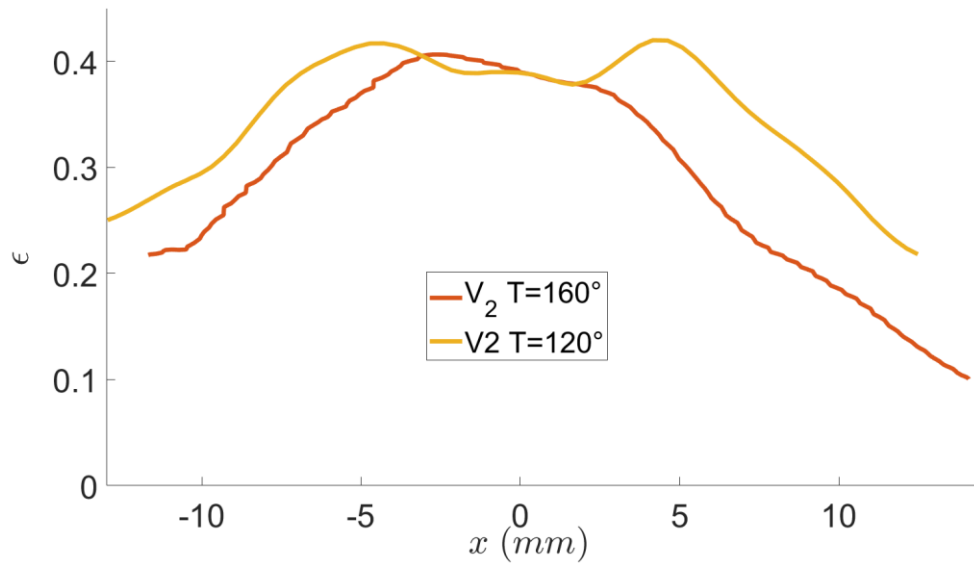


Figure S9 Strain profiles taken at 120°C and 160°C along the specimen central axis for the V_2 vitrimer. The measurements were made when the strain in the specimen center was $\varepsilon^M = 0.4$. At $T = 80^\circ\text{C}$, rupture occurred before the strain reached $\varepsilon^M = 0.4$ in the specimen center (see Figure S4 or Figure 8a).

6. Creep tests

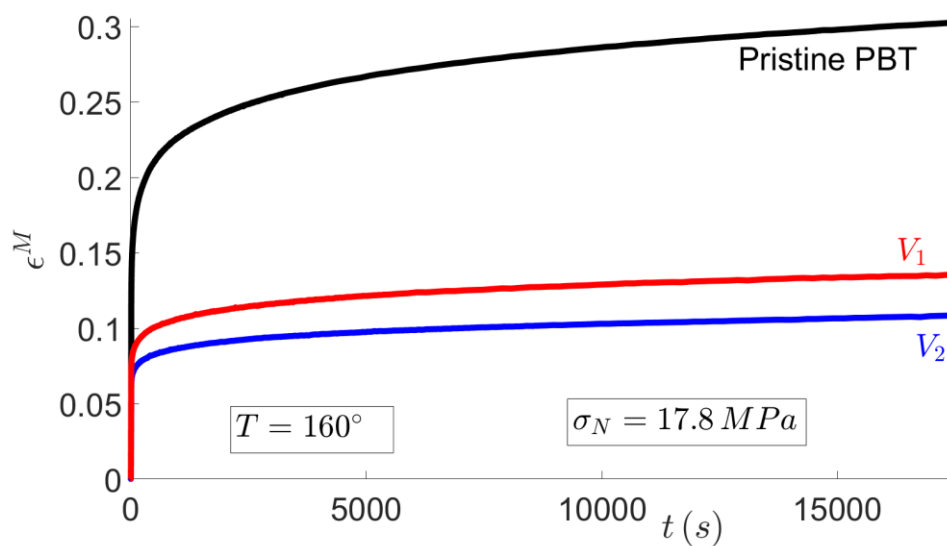


Figure S10 Creep experiments carried out during 4 hours.

7. Continuous Reactive Extrusion



Figure S11 Extruder blockage

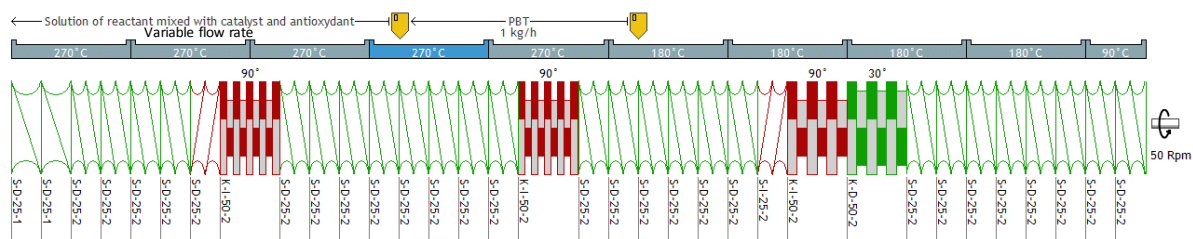


Figure S12 Screw and temperature profiles of the twin-screw extruder.

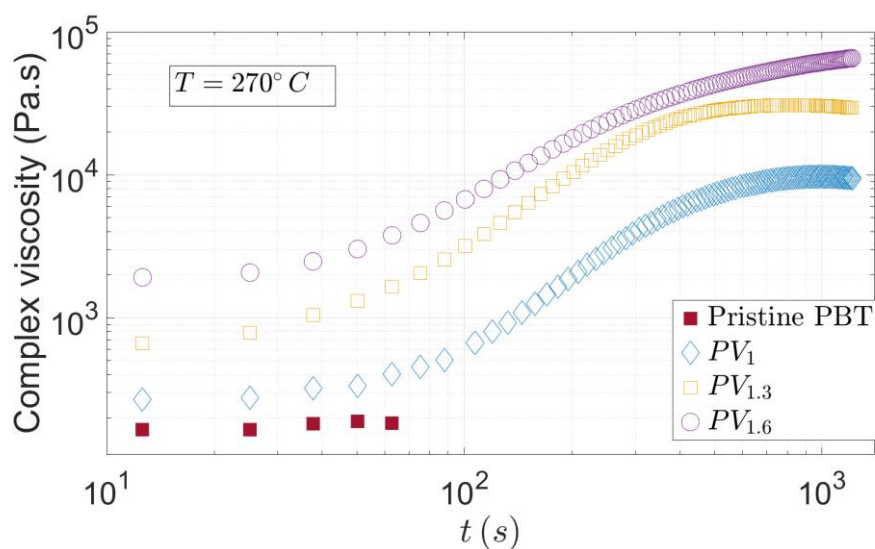


Figure S13 Time-dependence of the pre-vitrimer complex viscosities. The rheometer temperature is $T = 270^\circ\text{C}$.

References

- ⁱPyda, M., Nowak-Pyda, E., Mays, J., & Wunderlich, B. (2004). Heat capacity of poly (butylene terephthalate). *Journal of Polymer Science Part B: Polymer Physics*, 42(23), 4401-4411.
- ⁱⁱWeigand, S. J.; Keane, D. T. (2011) DND-CAT's new triple area detector system for simultaneous data collection at multiple length scales. *Nuclear Instruments and Methods in Physics Research*, A649, 61–63.
- ⁱⁱⁱDesborough, I. J.; Hall, I. H. (1977) A comparison of published crystalline structures of poly(tetramethylene terephthalate). *Polymer*, 18, 825-830.